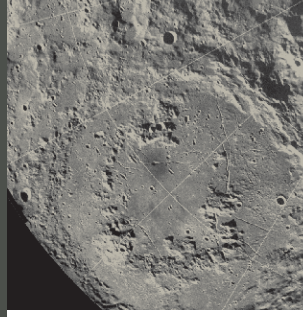


The Impact-Cratering Process

Gareth S. Collins[1], H. Jay Melosh[2] and Gordon R. Osinski[3]

1811-5209/12/0008-0025$2.50 DOI: 10.2113/gselements.8.1.25

Clementine mosaic of the ~320 km diameter Schrödinger peak-ring basin on the Moon. Peak-ring craters are so named because of the ring of discontinuous massifs that protrudes through the otherwise smooth impact deposits filling the crater floor. USGS SLIDE 18; NSSDC DATA SET, ID PHOTO: 94-004A-00E

Impact cratering is an important and unique geologic process. The high speeds, forces and temperatures involved are quite unlike conventional endogenic processes, and the environmental consequences can be catastrophic. Kilometre-scale craters are excavated and collapse in minutes, in some cases distributing debris around the globe and exhuming deeply buried strata. In the process, rocks are deformed, broken, heated and transformed in unique ways. Elevated temperatures in the crust may persist for millennia, and important chemical reactions are promoted by the extreme environment of the impact plume. Released gases may cause long-term perturbations to the climate, and impact-related phosphorus reduction may have played a role in the origin of life on Earth.

KEYWORDS: impact crater, crater collapse, ejecta, shock wave

INTRODUCTION

Impact cratering is a complex and dynamic process that operates on a range of spatio-temporal scales, from the micro-scale shock deformation of individual minerals to the mega-scale disruption and perturbation of planetary bodies. Current understanding of the processes involved comes from diverse disciplines, including geological mapping and remote sensing of the surface, geophysical imaging of the subsurface, laboratory-scale analogue experiments, real-scale computer simulations, isotopic and elemental geochemical analysis, and kilometre-scale structural mapping and interpretation of impact products. Comprehensive expositions of the many facets of impact cratering are given by Roddy et al. (1977), Melosh (1989) and French (1998). Here we present an overview of the major physical and chemical processes and products that occur in a hypervelocity impact, that is, when an object such as an asteroid or comet – the impactor – collides with a dense surface – the target – at a speed exceeding the speed of sound in both impactor and target materials.

THE IMPACT PROCESS

The impact-cratering process is conventionally divided into three stages: contact and compression, excavation, and collapse. These three stages are not discrete, yet each is dominated by different physical processes and thus is most easily described and understood separately. In the following, we mainly describe the simplified case of vertical impact on an airless planetary body without a surficial water layer or target heterogeneity. In reality, most impacts occur at an oblique angle: the percentage of impactors that strike at impact angles less than 60° and less than 30° to the target surface is 75% and 25%, respectively (Shoemaker 1962). Nevertheless, the vertical impact case is the best studied and serves as a useful exemplar of many of the processes common to all impacts.

On planetary bodies with an atmosphere, small, weak or fast-moving impactors can be decelerated, deformed, ablated and disrupted during atmospheric traverse, before striking the surface (Passey and Melosh 1980; Bland and Artemieva 2003). On Earth, atmospheric effects become insignificant for stony impactors greater than 60 m in size and for denser and stronger iron impactors greater than 20 m in size (Bland and Artemieva 2003). Fragments of impactors much smaller in size may reach the surface but only after being slowed considerably. Impact in a marine environment forms a crater in the water, generating large water waves. The movement of water can modify, inhibit or even suppress the cratering process on the seafloor (e.g. Wünnemann et al. 2010), leading to significant differences between marine and non-marine impact structures (Ormö and Lindström 2000).

Contact and Compression

Upon striking the target surface, the impactor decelerates as it compresses and pushes target material out of its path. At the contact of impactor and target, the rapid compression of both materials creates shock waves that propagate into the target and impactor (FIG. 1A). In contrast to conventional chemical processes, which occur at either constant pressure or constant temperature, the thermodynamic path traversed by highly shocked material starts with a sudden, irreversible compression that causes pressure to jump sharply to more than a few hundred gigapascals (GPa), accompanied by temperatures exceeding 10,000 K (FIG. 1A). For comparison, the pressure and temperature in Earth's core is ~350 GPa and ~5000 K, respectively. Under these extreme conditions, atomic bonds are easily broken and chemical rearrangements readily occur. After this brief compression, rarefaction (release) waves from free surfaces surrounding the high-pressure region propagate inward (FIG. 1B, C), permitting both the pressure and temperature to drop along a near-adiabatic path back to low pressure

1 Department of Earth Science and Engineering
Imperial College London, SW7 2AZ, United Kingdom
E-mail: g.collins@imperial.ac.uk

2 Department of Earth and Atmospheric Sciences
Purdue University, West Lafayette, IN 47907, USA
E-mail: jmelosh@purdue.edu

3 Depts. of Earth Sciences and Physics & Astronomy
University of Western Ontario, London, ON N6A 5B7, Canada
E-mail: gosinski@uwo.ca

(Fig. 1c, d), although temperatures may remain high enough to leave the material molten or even vaporized (Fig. 1e; Melosh 1989). In oblique impacts, the shock wave generated by the impact weakens with decreasing impact angle and becomes asymmetric, with the strongest shock in the downrange direction (Pierazzo and Melosh 2000).

The contact and compression stage ends when the release wave unloads the impactor from high pressure. The principal result of the contact and compression stage is the partitioning of most of the impactor's kinetic energy into the kinetic and internal energy of the target and impactor. The internal energy heats both the impactor and the target; the residual kinetic energy is spent displacing and ejecting target and impactor material, producing a crater in the target surface (Fig. 2).

Excavation and Ejecta Emplacement

As the (approximately) hemispherical shock wave in the ground continues to propagate away from the impact site, it attenuates and eventually degrades into a normal stress wave (Melosh 1989). Behind the shock wave, the residual velocity imparted by the shock acts to excavate and displace target material at speeds much slower than that of the shock wave (Fig. 2a). During early growth, an approximately hemispherical crater is formed (Fig. 2b), which may be elongated along the trajectory of the impactor if impact is sufficiently oblique. The growth of the crater is resisted by the residual strength of the target rocks and the weight of the displaced target material in the ambient gravity field (Holsapple 1993). In large hypervelocity impacts, including all those on Earth, gravity is the most significant factor.

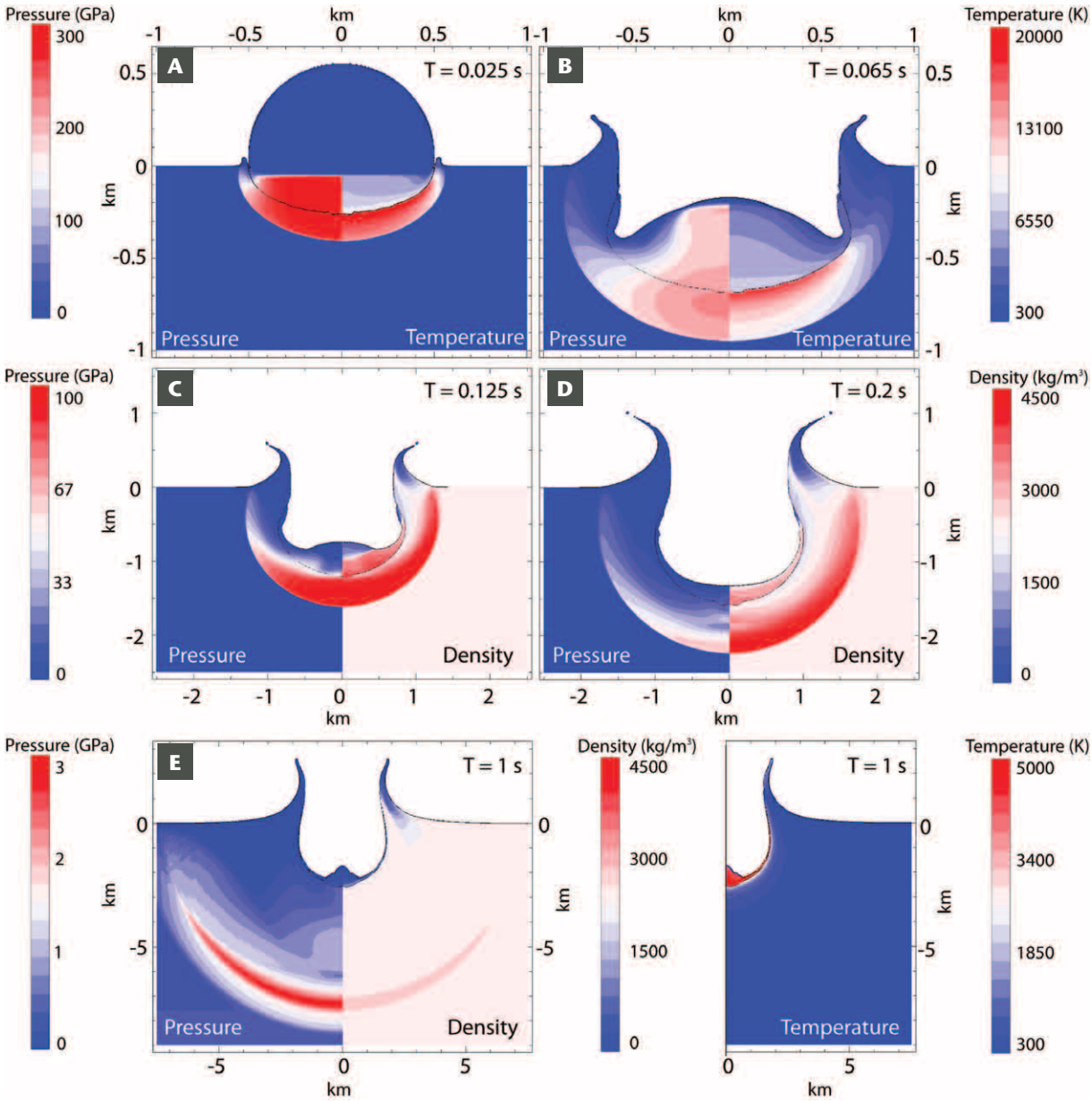


Figure 1 Contact and compression of the impactor as it strikes a target surface. Five snapshots are shown from a numerical impact simulation, between 0.025 and 1 second after initial contact, of a 1 km diameter dunite impactor striking a granite target at 18 km/s (the average impact velocity for asteroidal impactors on Earth). Note the change in the length, pressure and temperature scales between the rows. (**A**) Impactor just after contact with the target: A small region of high pressure develops along the interface. Both target and impactor are compressed and begin to distort in shape; the rear of the impactor is unaffected by events at the leading edge. (**B**) The shock wave in the impactor reaches its rear surface and (**C**) is reflected as a rarefaction (release) wave, unloading the impactor to low pressure. (**D**) The shock wave in the target propagates outward in an approximately hemispherical geometry, closely followed by the release wave. (**E**) Behind the detached shock wave, the impact plume (vaporized impactor and proximal target) begins to expand and the excavation flow is initiated.

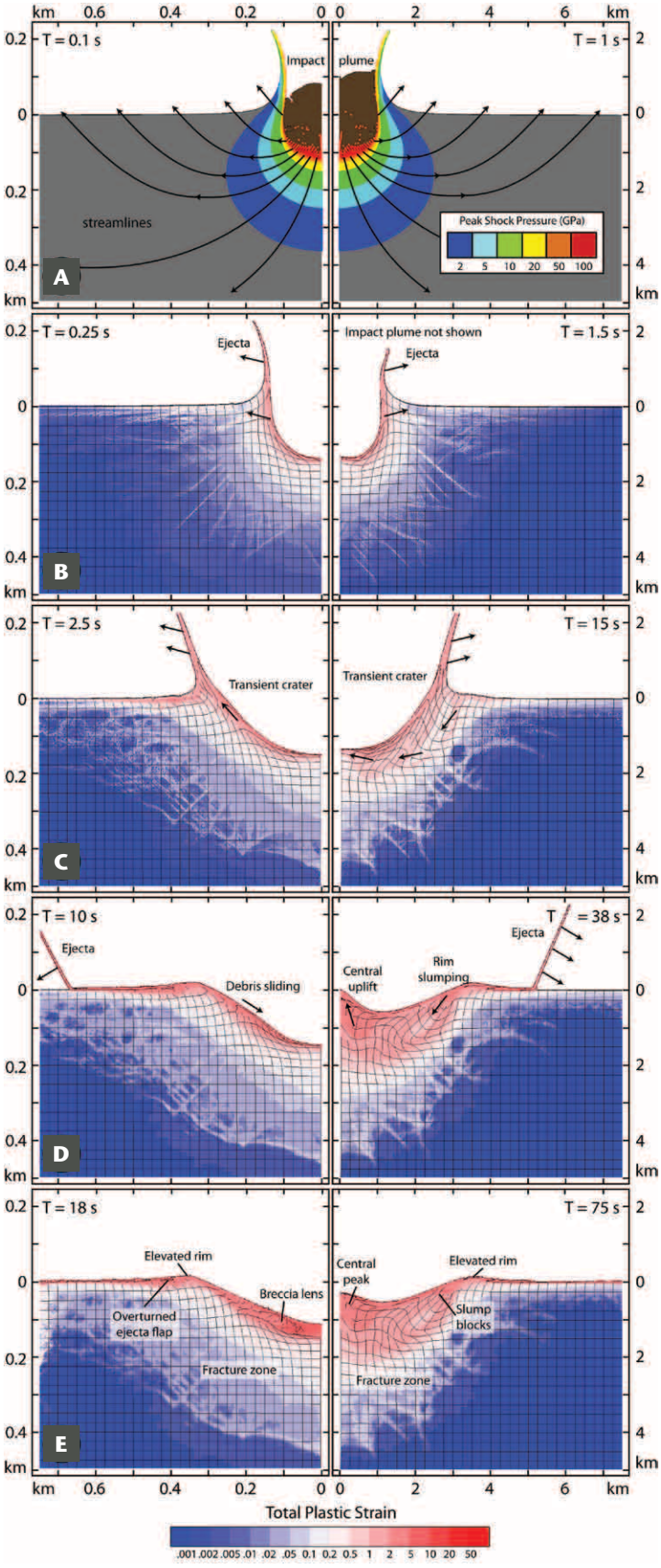


Figure 2 The excavation and collapse of simple and complex craters on Earth. Five snapshots at different times from numerical simulations of the formation of a simple crater (left) by a 50 m diameter impactor at 12 km/s, and a complex crater (right) by a 500 m diameter impactor at the same speed (note the different time and length scales in each scenario). Material parameters representative of non-porous sandstone (quartzite) were used to describe the target and impactor material response. (**A**) The excavation flow is initiated by the expanding shock wave. The coloured contours show peak pressure, which decreases in magnitude with distance from the impact point. The impact plume is shown in brown. (**B**) Time of maximum cavity depth. The grid lines show deformation in the target; the coloured contours show accumulated plastic strain. (**C**) The end of excavation and the onset of collapse. The geometry of the crater at this point is termed the "transient crater." (**D**) Collapse stage: the diameter of the crater continues to grow as the rim collapses inward by debris sliding in the simple crater example and by wholesale slumping in the complex crater case. In the simple crater example (left), the crater floor remains stable, whereas in the complex crater case (right), the crater floor rebounds to form a central uplift. (**E**) The final crater form.

At the end of crater growth, crater shape departs from a hemisphere, typically because downward motion of the crater floor stops before outward crater excavation ceases (Fig. 2c). In oblique impacts, asymmetries in crater shape are lost with increasing crater growth, but growth along different azimuths may be arrested at different times.

As the crater grows, a large volume of rock debris is ejected ballistically onto the surface surrounding the crater (Fig. 2d). The kinematics of the excavation flow implies that material ejected at a given radius contains a mixture of material exposed to different shock levels (Fig. 2b). Close to the crater rim, ejecta is deposited in a continuous blanket that interacts with the pre-existing surface (Oberbeck 1975); farther out, the ejecta lands as a scattered assortment of fine-grained dust and larger blocks, which may themselves excavate small secondary craters.

Unlike crater shape, the evolution of the ejecta curtain and deposition of ejecta are quite sensitive to impact angle when the angle is below 45° (Gault and Wedekind 1978). Characteristic ejecta morphologies have become diagnostic of oblique impact (Schultz 1992).

Collapse

The product of the excavation stage is a deep, bowl-shaped cavity, many times larger than the impactor, termed the transient crater or cavity (Fig. 2c) (Dence et al. 1977; Turtle et al. 2005). In highly oblique impacts, the transient crater may be elongated in the direction of impact, with a steepened interior wall in the uprange direction. Crater collapse, the subsequent and final stage of the cratering process, is the gravity-driven modification of the transient crater (Fig. 2d). In small craters, those less than approximately 4 km diameter on Earth, the steepest part of the rim collapses into the crater bowl to produce a breccia lens comprised largely of broken rock, but with some highly shocked and shock-melted material, in an otherwise unmodified transient crater (Fig. 2d, e; Fig. 3a) (Grieve et al. 1977). Such craters are called *simple craters* (Dence 1965) and have a final depth-to-diameter ratio of ~1:5 (Pike 1977).

Larger craters collapse more spectacularly, giving rise to central uplifts and slumped rim terraces (Fig. 2d, e; Fig. 3b). These are called *complex craters* (Dence 1965) and have a final depth-to-diameter ratio much less than 1:5. An important distinction between simple and complex crater collapse is that the latter involves substantial uplift of the crater floor and underlying strata (Fig. 2d); the maximum stratigraphic uplift is equivalent to approximately one-tenth of the final crater diameter (Ivanov et al. 1982).

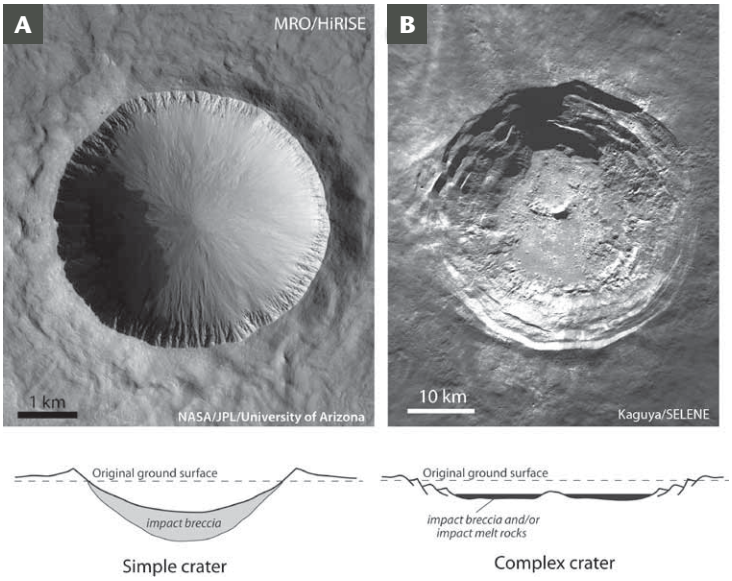


Figure 3 (**A**) HiRISE image of an unnamed simple crater on Mars (38.7° N, 316.1° E) displaying an elevated crater rim and steeply dipping upper cavity walls. The mid and lower parts of the wall are covered by talus deposits. (**B**) Kaguya/SELENE image (S0000001616_1906) of the complex impact crater Aristarchus on the Moon, showing a central peak, a flat crater floor with isolated hummocks and an extensive slump-terrace zone. Note the different scale bars in the two images.

On the Moon, central uplifts have been classified into several morphological types. So-called transitional craters represent the intermediate step between simple and complex craters; they typically display considerable crater-wall slumping, with minor faulting and terracing, but central uplifts are lacking. The smallest true complex craters display central peaks, comprising a peak, or series of peaks, that projects through the allochthonous crater-fill deposits. At larger diameters, the central peak disappears and, instead, peak-ring basins form. These craters, the best example of which is the lunar, 320 km diameter Schrödinger impact basin (see title-page image), possess a ring of peaks, often discontinuous, surrounding a central smooth depression infilled with impact melt–bearing crater-fill deposits. Unless buried almost immediately, terrestrial impact craters typically become modified from their original form over time. As such, the generic term *central uplift* is preferred.

Field observations and models suggest that central peaks form from the inward and upward movement of material within the displaced zone of the transient cavity. The formation of peak-ring basins is less well understood. One possible mode of origin is that in large complex craters, the central uplift may overshoot the ambient surface, before collapsing back downward and outward, on top of the inwardly collapsing crater rim, to form an internal peak ring (Collins et al. 2002).

The transition between simple and complex craters depends on 1/g, the inverse of the planet's surface gravity (Pike 1980), suggesting that collapse occurs when a strength threshold is exceeded (Melosh 1977). It also depends on target-rock strength, with the transition occurring at a diameter of ~4 km in crystalline and ~2 km in sedimentary target rocks in the terrestrial environment. The apparent strength of the target rock, however, is very low: only a few bars and with little or no internal friction. The physical explanation for this temporary strength degradation is not well understood, but may be acoustic fluidization (Melosh and Ivanov 1999) or some other dynamic fault-weakening mechanism.

IMPACT PRODUCTS

The combination of high stresses, strain rates and temperatures makes the impact process unlike any endogenic geological process. Sudden and brief exposure to extreme force and heat causes unique modifications to rocks and minerals, termed *shock metamorphic effects* (see French and Koeberl 2010; Langenhorst and Deutsch 2012 this issue). Most rocks affected by an impact are not heated significantly; they are simply deformed or broken and displaced. Shock alteration is more profound close to the actual point of impact, where the initial shock pressure and temperature are higher (see Langenhorst and Deutsch 2012).

The transport and mixing of impact-modified materials during the excavation and collapse stages of crater formation produce a wide variety of distinctive *impactites* (i.e. rock affected by impact metamorphism), which span a continuum from melt-free impact breccias (lithic breccias) to clast-poor impact melt rocks (Stöffler and Grieve 2007). These different impactite types may be found in a variety of settings within and around an impact crater. Some impactites, such as those comprising central uplifts and crater floors and rims, are largely in situ (termed autochthonous or parautochthonous), while others are transported tens of kilometres from their original stratigraphic position (termed allochthonous).

Impact melt–bearing impactites have been documented in four main settings: (1) large-scale continuous impact melt layers or "sheets" and/or smaller isolated bodies within the crater interior and rim region; (2) small, metre- to centimetre-scale, glassy (often devitrified or altered) particles, either within impact breccias or on their own, inside or outside the crater; (3) metre- to decametre-scale injection dykes in the crater floor and walls; (4) discrete millimetre- to centimetre-scale, glassy particles (spherules or tektites) distributed regionally to globally. Many of these impact melt–bearing impactites resemble volcanic rocks in the field and even under the microscope. At the Sudbury impact structure, Ontario, the impact melt sheet was so thick (~3 km) that it crystallized and differentiated to form rocks that were for a long time considered plutonic igneous rocks of endogenic origin (Grieve et al. 1991).

In terms of the products of impact melting, target lithology plays a fundamental role in determining their characteristics. Sedimentary rocks differ from crystalline rocks in several ways. In particular, they are typically richer in volatiles, have high porosity and are often layered. As a consequence, the products of impact melting in sedimentary rocks differ substantially in their appearance and characteristics (for example, they are typically more clast rich and contain mixtures of often immiscible melts generated from vastly different target rocks; Osinski et al. 2008). Nevertheless, impactites found in complex craters that were formed in sedimentary and mixed sedimentary–crystalline targets are very similar, which suggests that the impact-melting process is essentially the same in sedimentary and crystalline rocks (see Osinski et al. 2008 for a review).

Products and Processes of the Impact Plume

In a typical large impact, the impactor and a roughly equal volume of target rocks are melted and vaporized. This produces a turbulent mixture of vaporized rock, melt droplets, small solid fragments and, if an atmosphere is present, hot atmospheric gases, known variously as the *impact plume*, the *vapour plume* or (most dramatically) the "*fireball*". The impact plume rapidly expands from the impact site, carrying much of the impactor material with it, until it equilibrates with the surrounding atmosphere or breaches it completely and extends into space. The evolution and

deposition of impact plume material, as well as the concomitant chemical processing of plume constituents, are among the least well-understood aspects of the impact process, and yet it is this impact product that can have the most devastating effect on the local and global environment. For example, the global climatic effects that caused the Cretaceous–Palaeogene mass extinction are widely believed to be the direct result of an impact plume composed of dust, soot and climatically active gases injected into the atmosphere by the Chicxulub impact (Schulte et al. 2010; Pierazzo and Artemieva 2012 this issue).

Complex molecular solids, of which silicate rocks are a prime example, vaporize in a complex manner. Even the simplest silicate, SiO_2, decomposes into molecular fragments as temperature rises (Fig. 4). Up to a few thousand degrees above the vaporization temperature (about 3100 K at a pressure of 0.1 MPa), the principal molecules in silica vapour are SiO and O_2. At still higher temperatures, these diatomic molecules break down further, eventually yielding monatomic Si and O. At even higher temperatures, free electrons appear and the atoms are ionized. The same transitions occur at higher pressures, but they are pushed to higher temperature until, at a sufficiently high pressure and temperature, the critical point is passed, no liquid/vapour transition exists, and the very concept of discrete molecular clusters loses its meaning.

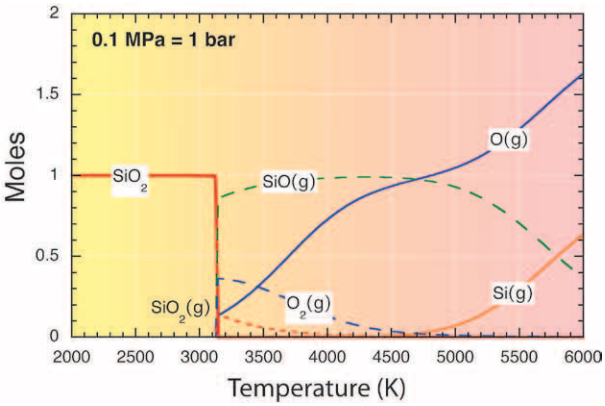


Figure 4 Species present in the vapour phase of SiO_2 as a function of temperature for a pressure of 0.1 MPa. The vapour phase is predominantly SiO plus O_2 just above the vaporization temperature, with an admixture of about 20 mole % of SiO_2. At higher temperatures these molecular clusters break down into atoms so that the high-temperature limit is a mixture of monatomic Si and O gases. Adapted from Melosh (2007)

Figure 5 illustrates several alternative thermodynamic paths experienced by shocked silica, SiO_2, as it decompresses. These are qualitatively similar to the shock behaviour of many other silicate materials (see Langenhorst and Deutsch 2012). During its initial release from high pressure, the shocked material is neither a liquid melt nor a gas: the pressure is higher than the critical pressure, approximately 0.19 GPa for SiO_2 (black dot), and so the material behaves as a single-phase hot fluid. As the pressure drops below the critical point the release path intersects the liquid–vapour phase curve (shown in green). Depending on the internal energy of the fluid, two outcomes are possible: either the fluid reaches the phase curve from the liquid side, in which case vapour bubbles appear in the liquid (boiling; blue curves), or it reaches the phase curve from the vapour side, in which case droplets of liquid melt condense from the gas (red curves). In either case a two-phase mixture suddenly appears. It is then possible for elements to exchange between phases, thus initiating chemical

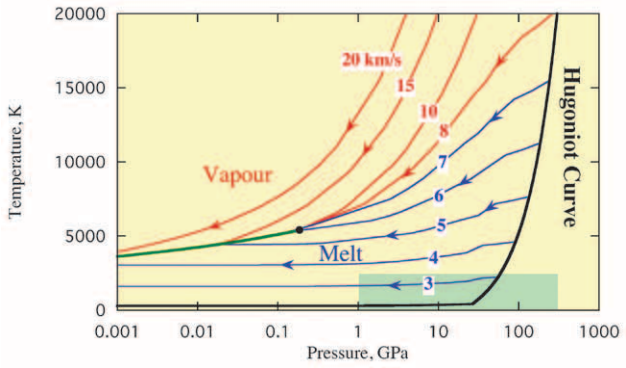


Figure 5 Thermodynamic paths of the adiabatic release of shocked SiO_2 from high pressure on a log P versus T diagram. The Hugoniot curve, shown as a thick black line, is the final result of increasingly strong shock compression of quartz, starting from an initial state of 0.1 MPa and 23 °C. The red and blue lines are decompression isentropes (release adiabats), which show the history of temperature and pressure of decompressing material. The phase curve separating liquid and solid phases is shown as a green line on the left of the plot, and the critical point is represented by the black dot. The numbers labeling the release adiabats are the particle velocities in the shocked material in kilometres per second, which can be interpreted as the outcome of an impact experiment between identical materials at twice the particle velocity. Thus, the curve labeled 7 is the release isentrope of a face-on impact between two quartz plates at 14 km/sec. The green rectangle encompasses the pressure and temperature range normally considered in terrestrial geology.

changes. Furthermore, the rapid cooling of the emulsion of liquid and vapour readily quenches high-temperature chemical equilibria and so preserves the high-temperature assemblage of chemical species.

The most characteristic chemical change resulting from impact is loss of oxygen or reduction of the melt phase, with complementary oxidation of the vapour phase. On Earth's surface, most rocks contain substantial amounts of oxidized iron, Fe^{3+}. However, the iron in the melted or condensed products of impact (e.g. tektites) is dominated by reduced iron, Fe^{2+}. On the Moon, where the pre-impact rocks contain mostly Fe^{2+}, impact-melted agglutinates contain large amounts of nanophase iron, Fe^0. The chemical reactions involved are:

$$Fe_2O_3\ (\text{melt}) \rightarrow Fe_2O\ (\text{melt}) + \frac{1}{2}O_2 \uparrow$$

$$Fe_2O\ (\text{melt}) \rightarrow Fe\ (\text{liquid}) + \frac{1}{2}O_2 \uparrow$$

where Fe_2O_3 and FeO are taken to be components of a silicate solution. Although the energy of the Fe–O bond might suggest that the above reactions should proceed to the left, the high entropy of the hot vapour phase drives them to the right.

In strong contrast to volcanic glasses, which in some cases may contain up to several weight percent water, tektites are strongly depleted in water, containing only about 10–100 ppm (cf Glass and Simonson 2012 this issue). Once a major mystery, the rapid loss of water (as well as volatile elements such as sodium and potassium) is now attributed to the extreme nature of impact heating.

In addition to iron, other species may be reduced. Of particular interest is phosphorus, which on Earth and in stony meteorites most commonly occurs in the oxidized 5+ state as part of the phosphate ion, PO_4^{3-}. Such phosphate, when added to a water solution of organic hydrocarbons and sugars, does little to produce the long phosphate polymers that typify RNA and DNA, or the doublets and triplets that characterize ADP and ATP.

However, when reduced phosphorus is added in the form of P^{3+} or P^0, reactions occur that produce many of the phosphate molecules found in all biological systems (Pasek 2008). But how is this reduced phosphorus produced? Pasek (2008) originally suggested that it might come from the mineral schreibersite, $(Fe,Ni)_3P$, a rare phase in some iron meteorites. But it now seems much more likely that meteoritic phosphorus was reduced by the impact itself, then scattered globally, dissolved in the glassy melt droplets produced by large impacts. This realization is now forging a close connection between impact chemistry and the origin of living organisms, highlighting the importance of understanding the chemical effects of high-speed impacts.

CONCLUSIONS

The high speeds, forces and temperatures involved in impact cratering produce unique rock modifications, large basins, uplifts and ejecta deposits. Impacts can also have catastrophic environmental consequences (e.g. Toon et al. 1997; Pierazzo and Artemieva 2012). Traditionally, impacts have not been viewed as agents of chemical change – their physical effects are far more obvious. Nevertheless, important chemical changes, such as molecular decomposition and volatile loss, do occur during the impact process, particularly in the impact plume. The release of climatically active gases, such as carbon dioxide, sulfur oxides and water vapour, can cause global perturbations to the climate. Moreover, as reduced phosphorus has been shown to produce many of the phosphate molecules found in biological systems, it is possible that as a reducing agent impacts have played a role in the origin of life on Earth.

ACKNOWLEDGMENTS

We thank Kai Wünnemann for the simulation results used to create Figure 2. This article benefited greatly from constructive reviews by Alex Deutsch and Peter Haines. GSC was funded by NERC Fellowship Grant NE/E013589/1.

REFERENCES

Bland PA, Artemieva NA (2003) Efficient disruption of small asteroids by Earth's atmosphere. Nature 424: 288-291

Collins GS, Melosh HJ, Morgan JV, Warner MR (2002) Hydrocode simulations of Chicxulub crater collapse and peak-ring formation. Icarus 157: 24-33

Dence MR (1965) The extraterrestrial origin of Canadian craters. Annals of the New York Academy of Sciences 123: 941-969

Dence MR, Grieve RAF, Robertson PB (1977) Terrestrial impact structures: Principal characteristics and energy considerations. In: Roddy DJ, Pepin RO, Merrill RB (eds) Impact and Explosion Cratering. Pergamon Press, New York, pp 247-275

French BM (1998) Traces of Catastrophe: A Handbook of Shock-Metamorphic Effects in Terrestrial Meteorite Impact Structures. Lunar and Planetary Institute, Houston, Texas, Contribution 954, 120 pp

French BM, Koeberl C (2010) The convincing identification of terrestrial meteorite impact structures: What works, what doesn't, and why. Earth-Science Reviews 98: 123-170

Gault DE, Wedekind JA (1978) Experimental studies of oblique impacts. Proceedings of the Lunar Planetary Science Conference 9: 3843-3875

Glass BP, Simonson BM (2012) Distal impact ejecta layers: Spherules and more. Elements 8: 43-48

Grieve RAF, Dence MR, Robertson PB (1977) Cratering processes: As interpreted from the occurrence of impact melts. In: Roddy DJ, Pepin RO, Merrill RB (eds) Impact and Explosion Cratering. Pergamon Press, New York, pp 791-814

Grieve RAF, Stöffler D, Deutsch A (1991) The Sudbury structure: Controversial or misunderstood? Journal of Geophysical Research 96(E5): 22753-22764

Holsapple KA (1993) The scaling of impact processes in planetary sciences. Annual Review of Earth and Planetary Sciences 21: 333-373

Ivanov BA, Basilevsky AT, Sazonoya LV (1982) Formation of the central uplift in meteoritic craters. Meteoritika 40: 60-81 (in Russian; English technical translation 1986, NASA TM-88427)

Langenhorst F, Deutsch A (2012) Shock metamorphism of minerals. Elements 8: 31-36

Melosh HJ (1977) Crater modification by gravity: A mechanical analysis of slumping. In: Roddy DJ, Pepin RO, Merrill RB (eds) Impact and Explosion Cratering. Pergamon Press, New York, pp 1245-1260

Melosh HJ (1989) Impact Cratering: A Geologic Process. Oxford University Press, New York, 245 pp

Melosh HJ (2007) A hydrocode equation of state for SiO_2. Meteoritics & Planetary Science 42: 2079-2098

Melosh HJ, Ivanov BA (1999) Impact crater collapse. Annual Reviews of Earth and Planetary Sciences 27: 385-415

Oberbeck VR (1975) The role of ballistic erosion and sedimentation in lunar stratigraphy. Reviews of Geophysics 13: 337-362

Ormö J, Lindström M (2000) When a cosmic impact strikes the sea bed. Geological Magazine 137: 67-80

Osinski GR, Grieve RAF, Collins GS, Marion C, Sylvester P (2008) The effect of target lithology on the products of impact melting. Meteoritics & Planetary Science 43: 1939-1954

Pasek MA (2008) Rethinking early Earth phosphorus geochemistry. Proceedings of the National Academy of Sciences 105: 853-858

Passey Q, Melosh HJ (1980). Effects of atmospheric breakup on crater field formation. Icarus 42: 211-233

Pierazzo E, Artemieva N (2012) Local and global environmental effects of impacts on Earth. Elements 8: 55-60

Pierazzo E, Melosh HJ (2000) Understanding oblique impacts from experiments, observations, and modeling. Annual Review of Earth and Planetary Science 28: 141-167

Pike RJ (1977) Size dependence in the shape of fresh impact craters on the Moon. In: Roddy DJ, Pepin RO, Merrill RB (eds) Impact and Explosion Cratering. Pergamon Press, New York, pp 489-509

Pike RJ (1980) Control of crater morphology by gravity and target type: Mars, Earth, moon. Proceedings of the Lunar and Planetary Science Conference 11: 2159-2189

Roddy DJ, Pepin RO, Merill RB (1977) Impact and Explosion Cratering. Planetary and Terrestrial Implications. Pergamon Press, New York, 1301 pp

Schulte P and 40 coauthors (2010) The Chicxulub asteroid impact and mass extinction at the Cretaceous–Paleogene boundary. Science 327: 1214-1218

Schultz PH (1992) Atmospheric effects on ejecta emplacement and crater formation on Venus from Magellan. Journal of Geophysical Research 97: 16183-16248

Shoemaker EM (1962) Interpretation of lunar craters. In: Kopal Z (ed) Physics and Astronomy of the Moon. Academic Press, London, pp 283-359

Stöffler D, Grieve RAF (2007) Impactites. In: Fettes D, Desmons J (eds) Metamorphic Rocks. Cambridge University Press, Cambridge, pp 82-92

Toon OB, Zahnle K, Morrison D, Turco RP, Covey C (1997) Environmental perturbations caused by the impacts of asteroids and comets. Reviews of Geophysics 35: 41-78

Turtle EP, Pierazzo E, Collins GS, Osinski GR, Melosh HJ, Morgan JV, Reimold WU (2005) Impact structures: What does crater diameter mean? Geological Society of Americal Special Paper 384: 1-24

Wünnemann K, Collins GS, Weiss R (2010) Impact of a cosmic body into Earth's ocean and the generation of large tsunami waves: insight from numerical modeling. Reviews of Geophysics 48: RG4006, 26 pp, doi:10.1029/2009RG000308